SUPPLEMENTARY INFORMATION
DOI: 10.1038/NGEO554

Southward movement of the Pacific Intertropical Convergence Zone AD 1400 to 1850

Julian P. Sachs, Dirk Sachse, Rienk H. Smittenberg, Zhaohui Zhang, David S. Battisti, Stjepko Golubic

Supplementary Information

Materials and Methods

Sediment sampling and treatment

Washington Lake (WL): Three sediment cores from the deepest basin were analyzed: one 85 cm long sediment-water interface core (WL2-MW2) and two long cores (WL1 and WL2) that penetrated to the coral basement at 9.3 and 7.3 m, respectively (Fig. 2). Sedimentation began around 1200 B.C. (Table S1). Sequential core sections (100 cm each) were obtained with a Livingstone-type rod-operated piston corer (Geocore, Columbus, Ohio), sealed in the field and kept refrigerated at 4°C until core splitting, imaging and sub-sampling. This coring device was adapted to fit a transparent PVC tube (54 mm OD) and a custom-made rubber piston allowing intact recovery of the fragile uppermost part of the sediment-water interface. The same device was used in each of the three locations in this study. Sediment-water interface cores were subsampled on site in 1 cm intervals and frozen the same day.

Christmas Island (CI): Lake F6 (1°51' 5" N, 157°24' 34" W; surface area 0.16 km^2) showed little chemical or physical variation through the 6.1 m-deep water column[1]. A 92 cm surface core was recovered that contained thick, red, gelatinous, living microbial mat and the underlying buried mat material (Fig. 2k). An intact mat was recovered by hand and sampled into visually distinct color layers for microscopy (Fig. 2l,m,n).

Spooky Lake, Palau (SL): a sediment-water interface core was recovered from the center of the eastern-most basin in 12 m of water.

El Junco, Galápagos (EJ): Sediments used in this study are from a sediment-water interface core (EJ7-MW1) recovered from the center of the lake, and from a nearby 3.5 m core obtained with a

DOI: 10.1038/NGEO554

9-cm-diameter Nesje piston corer by colleagues from the University of Arizona. The latter was stored at 4°C until sub-sampling into 0.5 cm intervals. Some bioturbation was observed in the cores, presumably smoothing out individual ENSO events and limiting the resolution to a decadal time scale.

All sediment sub-samples from the various lakes were frozen after sectioning, freeze-dried and ground to a fine powder before chemical analysis. SL samples were passed through a 2 mm sieve to separate macrofossils.

Dating and age models

^{210}Pb (46.5 keV) and ^{214}Pb (295 and 352 keV) were measured in dried sediments from the SL and EJ interface cores on a low-energy germanium detector (Canberra Instruments). Counter efficiency was calibrated with sequential additions of known amounts of standard pitchblend. Unsupported ^{210}Pb was calculated by subtracting supported ^{210}Pb, which is in equilibrium with ^{214}Pb, from total ^{210}Pb. A ^{210}Pb chronology was constructed assuming constant rate of supply (CRS) and by relating the exponential ^{210}Pb decay profiles with the cumulative dry mass – depth profiles as determined using bulk density measurements (EJ, SL) and using a CRS computer model (EJ)[2]. Age models for EJ and SL were constrained by radiocarbon analyses that indicated nuclear-bomb-test-derived ^{14}C in the upper sediments, assumed to correspond to the early 1960s (Tables S2 and S4).

The ^{210}Pb-based age model for Spooky Lake was extended using the radiocarbon content of terrestrial plant material from 63 cm that had a calibrated age[3,4] between 1415-1450 A.D. (Table S2). Modeled ages contain an uncertainty ranging from a few years at the top of the core to a few decades at the bottom of the core, reflecting the uncertainties of the dating methods.

The age model of El Junco Lake was constructed with OxCal 4.0.1 beta software[5], incorporating both CRS modeled ^{210}Pb ages and radiocarbon dates of bulk sediments from EJ7-MW1 and the Nesje core (Table S3), adopting the Southern Hemisphere 2004 calibration curve[6] and the

P_sequence model with k=1 cm^{-1}. Sediment ages between dated samples were linearly interpolated. Modeled ages contain an uncertainty ranging from a few years at the top of the core to a few decades at the bottom of the core (Tables S3 and S4). Any reservoir effect that might influence the radiocarbon ages is unlikely since: (i) there are no carbonate rocks in the small volcanic crater in which the lake sits, (ii) the lake is shallow (6 m) and well mixed, (iii) the lake is unlikely to receive carbonate from sea spray since it is at 750 m elevation, under a stable atmospheric inversion much of the year, and close to the equator where storms are rare.

The Washington Lake age model is almost fully discussed in the main text methods section. The radiocarbon ages for the organic fraction in authigenic carbonate section (unit IV) are calibrated with both the atmospheric and the full marine calibration curve (Table S1), since it is not clear to what extent the lagoon was open to exchange with open sea.

Lipid extraction and δD analysis

Sediment samples were lyophilized and extracted with organic solvents using an automated solvent extractor. Subsequently, semi-pure fractions containing the compounds of interest were obtained using gravity column chromatography and/or High Pressure Liquid Chromatography (HPLC). Hydrogen isotope ratios were measured by Isotope Ratio Mass Spectrometry interfaced with either a thermal conversion elemental analyzer (TLE's) or gas chromatograph with pyrolysis furnace (lipids). Details about the hydrogen isotope analysis of total lipid extracts from microbial mats (CI) and sediments (WL, CI) is described in ref. 7. Details on the lipid extraction, purification and compound-specific hydrogen isotope analysis of botryococcenes (EJ) and dinosterol (SL) are described in refs. 8,9 and 10.

Water δD analysis

Lake and ocean water δD values from Palau were analyzed with the method described in ref. 9. Precision of water δD measurements was 0.5‰.

Supplementary Discussion

DOI: 10.1038/NGEO554

Additional influences on the hydrogen isotopic composition of total lipid extracts from Washington Lake microbial sediments

Species-specific differences in isotopic fractionation. Species-dependant differences in the isotopic fractionation during biosynthesis or water uptake are unlikely to be responsible for the observed differences in δD values. Despite changes in microbial assemblage along the salinity gradient on Christmas Island, including the two groups recognized in the Washington Lake core, the slope of the D/H fractionation (α) vs. salinity relationship did not change[7]. Furthermore, the response of total lipid extract (TLE) δD values to salinity was comparable to the response of individual compounds, also indicating a negligible effect of species-specific differences[7]. Microscopic evidence suggests a strong similarity between Christmas Island microbial mats and the Unit II-III Washington lake sediments. Therefore an effect of species-specific variations in the relationship is equally unlikely to be of major importance in the Washington Island microbial sediments.

Influence of plant-derived lipids. A larger contribution of plant lipids to the sediment below 260 cm (inferred from increasing plant debris below that depth) would tend to increase TLE δD values because vascular plant lipids tend to be enriched in deuterium by 30 to 60 ‰ compared to aquatic lipids[11] owing to leaf water isotopic enrichment during evapotranspiration. However, in Unit III, where plant remains were visible, we observed more negative TLE δD values. Additional support for our assumption of negligible land plant lipid input to unit II and III comes from $\delta^{13}C$ values of the sediment (Table S1). Values between -10.0 ‰ in unit II to -15.1 ‰ in unit III are typical for microbial organic matter in hypersaline environments where high productivity results in the depletion of aqueous CO_2 from the water[12,13] and exceeds the values observed in modern microbial assemblages on Kiritimati[14]. Though C_4 plants, such as many tropical grasses, have $\delta^{13}C$ values of around -15‰, the plant sample at 571 cm in Washington Lake sediment had a $\delta^{13}C$ value of -30.1‰ (Table S1). This low $\delta^{13}C$ value implies that plant-derived lipids could not have been substantial contributors to Unit II-III TLEs.

Further discussion on the use of dinosterol δD values from Spooky Lake, Palau,

As mentioned in the main text, δD values of algal lipids have proven to be very good recorders of water δD[9,11,15,16]. However, the same lipids from different organisms as well as different lipids from the same organism can express different isotopic fractionations against source water[9]. Thus, lipid biomarkers with as much algal source specificity are desirable for paleohydrological reconstructions with hydrogen isotopes. Dinosterol is produced almost exclusively by dinoflagellate algae[17] and is therefore assumed to be largely unaffected by the above-mentioned source-related effects. Possible changes in isotopic fractionation caused by growth rate[18] are likely to be small since the range of light and nutrient changes that may have altered dinoflagellate growth rates in Spooky Lake during the last 500 years were likely to have been too small to contribute substantially to the 30‰ signal we observe.

Dinosterol δD values may also have been influenced by salinity changes, as observed in Christmas Island's hypersaline ponds[7]. If that were the case, the salinity effect would work as an amplifier: less precipitation results in higher surface water δD values due to increased mixing with deuterium-enriched seawater and more D-enriched rain from a diminished amount effect[19]. Higher salinity would cause diminished D/H fractionation during lipid synthesis, resulting in more positive lipid δD values. For example, if salinity in the lake surface declined from 29 to 20 psu at the end of the LIA, the maximum amount possible assuming June 2004 deep and surface water values, respectively, and no salinity gradient in Spooky Lake during the LIA (i.e., that surface and deep waters had a salinity of 29 psu), only 6‰ of the 30‰ drop in dinosterol δD values at the end of the LIA could be attributed to the direct influence of salinity on D/H fractionation using the empirical relationship from Christmas Island[7].

The relative importance of (i) changes in rain water δD due to the amount effect, (ii) the extent of mixing between surface and subsurface water (that influences both the δD and salinity values of surface water), and (iii) the effect of salinity on D/H fractionation in dinosterol, cannot be determined from the dinosterol δD signal. Central to our argument, however, is the fact that the three mechanisms act in the same direction, driving dinosterol δD values higher in a diminished

DOI: 10.1038/NGEO554

rainfall regime, and lower during an enhanced rainfall regime. Thus dinosterol δD values can be used as a sensitive qualitative proxy for precipitation in Palau.

Correlation between the Southern Oscillation Index (SOI) and dinosterol δD values

In the upper Spooky Lake sediment the sampling interval of 1 cm is equivalent to approximately 5 yr. Regression of dinosterol δD values against 5-year averaged monthly values of the SOI (Table S6)[20] yields a significant anti-correlation where dinosterol δD increases by 3‰ for each 0.1 unit drop of the SOI (Fig. S1). Low SOI values correspond to El Niño conditions that are associated with drier conditions in the WPWP. Decreased shower intensity results in higher rain δD values (via the amount effect), less stratification resulting in more mixing of surface water with D-enriched and saline subsurface water, and hence higher surface water δD values that are recorded by dinosterol δD values. To the extent that D/H fractionation in dinosterol decreases at higher salinities in brackish water, the effect of diminished rainfall would be amplified in the dinosterol δD values.

Supplementary Figures

Fig. S1. Regression of Dinosterol δD and 5 year-averaged instrumental SOI values[20]. Values and 1σ error bars as listed in Table S6.

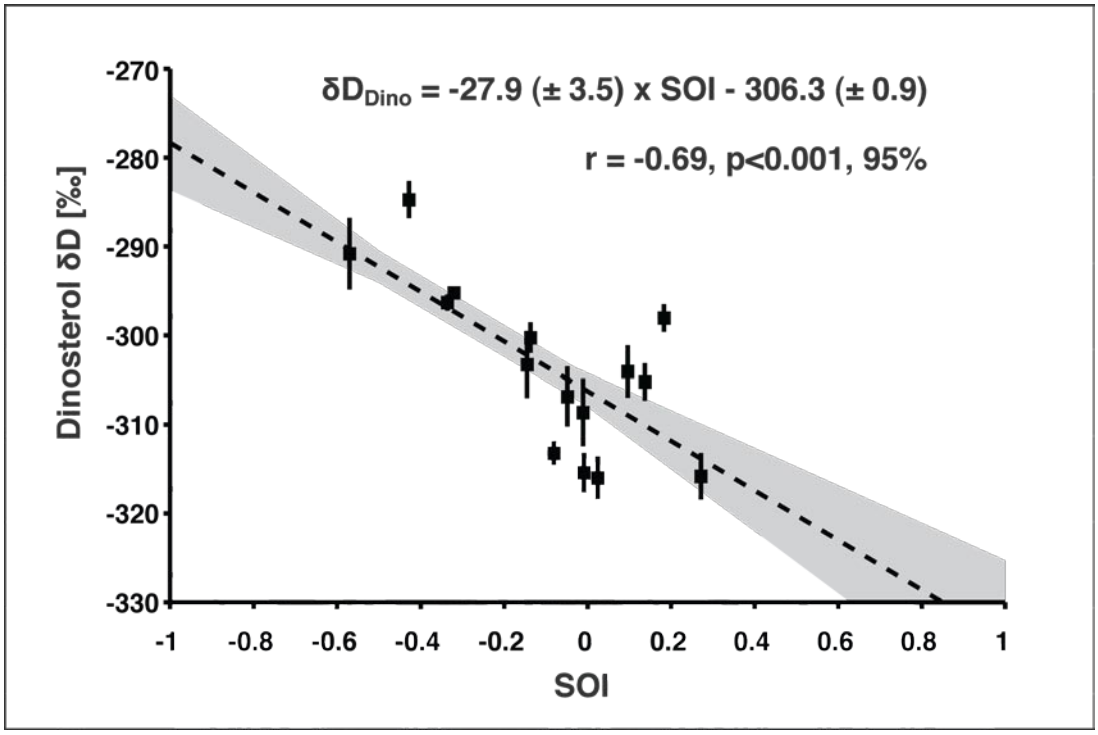

DOI: 10.1038/NGEO554

Supplementary Tables

Table S1. Radiocarbon ages and contents from Washington and Christmas Island sediments. a) Core codes as described in the text. Christmas Island mats as described in ref. 1. b) TOC = Total Organic Carbon of bulk sediment. c) Radiocarbon content for modern samples expressed as percent modern Carbon (pMC). d) Age ranges obtained by use of the atmospheric calibration curve[3] and their probability distribution. e) Age ranges obtained by use of a mixed calibration curve with a 15 ± 5 % marine contribution[21], applying the reservoir age correction of nearby Fanning Island[22] (i.e. a reservoir age of around 314 yr) and 85% from the atmosphere[3], and their probability distribution. f) Modeled ages constructed using OxCal 4.0.1 beta[5], with the *P_sequence* model and k=0.1 cm^{-1} (*a*): based on atmospheric calibration; (*b*): based on mixed calibration. g) Expressed against the Vienna Pee Dee Belemnite (VPDB) standard. h) LL: Lawrence Livermore National Laboratory, Livermore, CA, USA; IN: INSTAAR, University of Colorado, Boulder, CO, USA; NO: NOSAMS, Woods Hole Oceanographic Institution, Woods Hole, MA, USA. n.d.= not determined. s.e. = standard error. *Calibrated using a 100% marine calibration curve[21].

Core [a]	Sample type [b]	Depth (cm)	^{14}C age (yr BP / pMC) [c]	s.e. (±)	A - Cal Range (yr BP) [d]	Prob (%)	M- Cal range (yr BP) [e]	Prob (%)	Oxcal Model age (yr AD) [f]	δ^{13}C (‰) [g]	Lab [h]
WL 1	TOC	33	104 pMC	0.4	modern					n.d.	LL
MW 2	TOC	83	109 pMC	0.2	modern					-14.0	IN
WL 1	TOC	101	110 pMC	0.4	modern					n.d.	LL
WL 2	TOC	111	107 pMC	0.4	modern					-12.9	IN
WL 2	TOC	112	305	15	430-411 332-305	72 24	422-399 318-268 170-150	3 76 17	1561 (*a*) 1646 (*m*)	-10.0	IN
WL 2	TOC	216	545	15	625-606	18	540-525	96	1417 (*a*)	-12.4	IN

Core [a]	Sample type [b]	Depth (cm)	^{14}C age (yr BP / pMC) [c]	s.e. (±)	A - Cal Range (yr BP) [d]	Prob (%)	M- Cal range (yr BP) [e]	Prob (%)	Oxcal Model age (yr AD) [f]	δ^{13}C (‰) [g]	Lab [h]
					558-524	78			1422 (*m*)		
WL2	TOC	321	555	25	635-494 562-522	43 53	(620) 554-490	<0.1 96	1309 (*a*) 1330 (*m*)	-14.9	NO
WL 1	TOC	530	940	15	920-796	96				-15.2	IN
WL 2	TOC	536	1065	15	1051-1032 1214-1178	11 85	968-900 854-830	92 4	909 (*a*) 1000 (*m*)	-15.1	IN
WL 2	plant fossil	571	1285	15	1280-1221 1214-1178	56 40			760 *(a)*	-30.1	IN
WL 1	TOC	630	2115	15	2147-2041	92	1765-1580 *	96		-17.7	IN
WL 1	TOC	930	2965	15	3211-3078	96	2767-2680 *	96		-13.3	IN
Christmas Island microbial mat surface grab samples											
F6-MW2	TOC	6-7	111 pMC	0.5	modern						LL
K31-MW1	TOC	9-10	103 pMC	0.4	modern						LL
K101	TOC	14-15	105 pMC	0.4	modern						LL

DOI: 10.1038/NGEO554

Table S2. ^{210}Pb activity (unsupported), cumulative dry mass and modeled ages of Spooky Lake, Palau sediments. a) The modeled ages, based on the bulk density and ^{210}Pb measurements, are constrained by radiocarbon analysis of plant remains (INSTAAR, University of Colorado, Boulder, CO, USA), indicating deposition before (-) or after (+) atmospheric nuclear bomb testing in the early 1960's. b) Radiocarbon age (NOSAMS, Woods Hole, USA) and calibrated age range (2σ) of terrestrial plant remains from the bottom of the core. n.d.= not determined. dpm/g = decays per minute per gram dry sediment.

Depth (cm)	^{210}Pb activity (dpm/g) (±4)	Cum. dry mass (g / cm^2)	Modeled age (yr AD) [a]
0-1	77.1	0.013	2001
1-2	102.7	0.039	1996
2-3	98.2	0.066	1990
3-4	79.3	0.093	1984
6-7	63.9	0.180	1966 (+)
8-9	52.0	0.241	1954
9-10	n.d.	0.272	1948 (-)
10-11	32.8	0.304	1941
13-14	29.1	0.404	1922
18-19	4.52	0.583	1888
		^{14}C age (yr BP)	Cal range (yr AD)
63-64 [b]	n.d.	470 ± 25	1415- 1451

Table S3. ^{210}Pb activity, cumulative dry mass and modeled ages of El Junco Lake, Galápagos sediments. a) The modeled ages, based on the bulk density and ^{210}Pb measurements, are constrained by radiocarbon analysis of bulk sediment (INSTAAR, University of Colorado, Boulder, CO, USA), indicating deposition before (-) or during / after (+ / ++) atmospheric nuclear bomb testing in the early 1960's. dpm/g = decays per minute per gram dry sediment.

Depth (cm)	^{210}Pb activity (dpm / g) (± 4)	Cum. dry mass (g / cm^2)	Modeled age [a] (yr AD)
0.5	122.827	1.88	2001
1.5	113.289	3.47	1996
2.5	106.224	5.13	1991
3.5	91.929	6.47	1986
4.5	78.059	7.73	1982 (++)
5.5	71.923	9.16	1977
6.5	66.460	10.56	1972
7.5	64.847	12.31	1964 (++)
8.5	68.224	13.64	1957 (+)
9.5	61.902	15.05	1947
10.5	41.017	16.52	1936 (-)
11.5	23.328	18.35	1924
12.5	18.826	20.30	1910
13.5	17.452	21.85	1897
14.5	18.368	23.21	1877

DOI: 10.1038/NGEO554

Table S4. Radiocarbon ages of El Junco Lake, Galápagos sediments. a) A composite core depth was adopted for both cores. b) N = Nesje piston core, E = EJ7-MW1 mud-water interface core. c) AA= Arizona AMS Laboratory, Tucson, AZ, USA; IN = INSTAAR, University of Colorado, Boulder, CO, USA. d) ^{14}C ages of bulk organic material. e) Calibrated age ranges (2σ) using the Southern Hemisphere 2004 calibration curve. f) Modeled ages (2σ) were constructed using OxCal 4.0.1 beta [ref 5], with the *P_sequence* model and k=1 cm^{-1}. Sediment ages were linearly interpolated between dated samples.

Depth (cm) [a]	Core [b]	Lab [c]	^{14}C Age (yr BP)[d]	s.e. (±)	$\delta^{13}C$ (‰)	Cal. Age (yr A.D.) [e]	OxCal modeled age (yr A.D.) [f]
44	N	AA	455	38	-28.8	1421-1622	1468-1616
50.5	E	IN	400	25	-27.2	1425-1624	1420-1509
64	N	AA	707	43	-27.9	1278-1394	1239-1370
84	N	AA	1171	40	-26.3	883-990	909-994
104	N	AA	1235	42	-26.5	715-976	678-815
144	N	AA	1885	40	-25.4	76.5-323	59-216

Table S5. Total lipid extract δD values and inferred salinities from Washington Lake. Salinity was calculated using the relationship salinity = (δD_{TLE} + 207) / 0.72 [ref 7]. δD is expressed relative to the Vienna Standard Mean Ocean Water (VSMOW). Most values are averages of three replicate measurements with the standard deviation (1σ) listed. Ages are linearly interpolated between ^{14}C control points and based on calendar ages calibrated with (a) atmospheric calibration curve, or (b) the mixed curve, as discussed in the text and listed in Table S1 and Fig. 3.

Depth (cm)	Sed. Unit	Age (yr AD) [a]	Age (yr AD) [b]	TLE δD (‰)	1σ	Inferred salinity (psu)
112-113	IIa	1559±34	1643±21	-145.1	3.5	86
113-114	IIa	1558±34	1641±21	-154.0	1.0	74
114-115	IIa	1556±34	1639±21	-139.8	2.9	93
115-116	IIa	1555±34	1637±21	-138.4	1.8	95
116-117	IIa	1554±34	1635±21	-151.6	1.0	77
117-118	IIa	1552±33	1633±21	-136.4	3.2	98
130-131	IIa	1534±31	1605±21	-130.8	2.2	106
131-132	IIa	1533±31	1602±21	-131.1	3.7	105
132-133	IIa	1532±31	1600±21	-139.4	1.1	94
133-134	IIa	1530±30	1598±21	-138.2	4.7	96
135-136	IIa	1527±30	1594±21	-134.9	1.9	100
136-137	IIa	1526±30	1592±21	-125.6	1.1	113
144-145	IIa	1515±28	1574±21	-130.8	6.0	106

DOI: 10.1038/NGEO554

Depth (cm)	Sed. Unit	Age (yr AD) [a]	Age (yr AD) [b]	TLE δD (‰)	1σ	Inferred salinity (psu)
172-173	II	1476±23	1514±21	-119.6	0.2	121
215-216	II	1417±15	1422±21	-116.0	5.6	126
253-254	III	1378±16	1388±21	-169.9	3.4	52
294-295	III	1337±16	1352±21	-162.0	4.1	63
324-325	III	1302±18	1326±21	-157.7	3.6	68
352-353	III	1249±18	1281±21	-147.8	1.4	82
381-382	III	1195±18	1237±22	-149.0	4.2	81
423-424	III	1117±18	1174±23	-153.6	3.0	74
441-442	III	1083±17	1146±23	-149.1	-	80
476-477	III	1018±17	1093±24	-154.9	4.0	72
499-500	III	975±17	1050±24	-160.9	1.3	64

Table S6. Dinosterol δD values from Spooky Lake, Palau and 20th century SOI values. D values are expressed against VSMOW. 1σ is the standard deviation of "n" replicate analyses. Listed ages are modeled ages and contain an uncertainty ranging from a few years (top) to a few decades (bottom) (Table S2). a) 5-year averaged values of the SOI [20], with the center year corresponding to the associated sediment age, which was used in Fig. S1.

Depth (cm)	Age (yr AD)	Dinosterol δD (‰)	1 σ	n	SOI [a]
2-3	1994	-290.8	4.2	5	-0.57
3-4	1989	-284.7	2.4	3	-0.43
4-5	1985	-296.3	1.1	3	-0.34
5-6	1980	-295.2	0.2	3	-0.32
6-7	1976	-298.1	1.7	4	+0.18
7-8	1971	-315.8	-	1	+0.27
8-9	1966	-313.2	1.4	4	-0.08
9-10	1961	-315.4	2.4	4	-0.01
11-12	1951	-308.7	4.4	3	-0.01
12-13	1946	-306.9	3.5	6	-0.05
13-14	1941	-303.3	4.4	3	-0.15
14-15	1935	-304.1	3.2	4	+0.10
15-16	1930	-316.0	2.8	3	+0.02
17-18	1918	-305.2	2.4	3	+0.14
20-21	1900	-300.3	1.9	4	-0.14
25-26	1868	-313.4	4.7	4	
37-38	1832	-302.6	6.6	6	
42-44	1793	-293.0	4.3	3	
47-48	1750	-298.7	2.5	3	
52-53	1704	-288.3	4.7	4	
58-59	1654	-286.0	5.9	3	
65-66	1579	-291.1	4.5	5	
70-71	1521	-290.2	5.0	5	

DOI: 10.1038/NGEO554

Table S7. Botryococcene δD values from El Junco Lake, Galápagos. δD values are expressed relative to VSMOW. 1σ is the standard deviation of "n" replicate analyses. Listed ages are modeled ages and contain an uncertainty ranging from a few years (top) to a few decades (bottom) (Tables S3 and S4).

Depth (cm)	Age (yr AD)	Botryococcene δD (‰)	1 σ	n
0-1	2001	-242.1	2.5	3
2-3	1991	-239.3	1.1	3
4-5	1982	-237.5	6.3	3
5-6	1977	-237.3	0.2	3
7-8	1964	-229.6	2.3	3
8-9	1957	-233.2	4.8	3
9-10	1947	-231.3	-	1
10-11	1936	-234.8	2.2	3
11-12	1924	-227.0	-	1
12-13	1910	-230.7	-	1
13-14	1897	-228.6	-	1
14-15	1885	-223.9	3.4	3
15-16	1873	-225.1	2.2	3
17-18	1850	-239.3	2.2	3
18-19	1838	-242.6	1.6	3
19-20	1827	-258.3	2.6	3
20-21	1815	-256.1	1.1	3
21-22	1804	-259.7	2.8	3
24-25	1769	-259.1	2.6	3
27-28	1734	-271.2	1.9	3

Depth (cm)	Age (yr AD)	Botryococcene δD (‰)	1 σ	n
30-31	1699	-267.5	1.4	3
33-34	1663	-264.2	0.3	3
36-37	1629	-265.1	2.0	3
39-40	1595	-268.6	1.9	3
44-45	1536	-280.7	0.9	3
49-50	1476	-270.3	0.4	3
54-55	1417	-266.5	1.5	3
59-60	1358	-277.7	1.4	3
64-65	1296	-280.2	0.1	3
69-70	1207	-283.6	0.5	3
74-75	1128	-266.8	3.1	3
79-80	1039	-254.7	1.0	3
83.5-84.5	951	-249.5	1.7	3
88.5-89.5	900	-255.6	2.8	3
93.5-94.5	849	-257.0	4.3	3
98.5-99.5	797	-245.0	3.9	3

DOI: 10.1038/NGEO554

Supplementary References

1. Saenger, C., Miller, M., Smittenberg, R., & Sachs, J. A physico-chemical survey of inland lakes and saline ponds: Christmas Island (Kiritimati) and Washington (Teraina) Islands, Republic of Kiribati. *Sal. Syst.* **2**, 8 (2006).

2. Appleby, P. G. & Oldfield, F. The calculation of lead-210 dates assuming a constant rate of supply of unsupported ^{210}Pb to the sediment. *Catena* **5**, 1-8 (1978).

3. Reimer, P.J. et al. IntCal04 terrestrial radiocarbon age calibration, 0-26 Cal Kyr BP. *Radiocarbon* **46**, 1029-1058 (2004).

4. Stuiver, M. & Reimer, P.J. Extended ^{14}C data base and revised CALIB 3.0 ^{14}C Age calibration program. *Radiocarbon* **35**, 215-230 (1993).

5. Bronk Ramsey, C. Deposition models for chronological records. *Quat. Sci. Rev.* **27**, 42-60 (2008).

6. McCormac F.G. et al. Radiocarbon Calibration from 0-26 cal kyr BP - SHCa104 Southern Hemisphere Calibration, 0-11.0 cal kyr BP. *Radiocarbon* **46**, 1087-1092 (2004).

7. Sachse, D. & Sachs, J. P. Inverse relationship between D/H fractionation in cyanobacterial lipids and salinity in Christmas Island saline ponds. *Geochim. Cosmochim. Acta* **72**, 793-806 (2008).

8. Zhang, Z., Metzger, P., & Sachs, J. P. Biomarker evidence for the co-occurrence of three races (A, B and L) of *Botryococcus braunii* in El Junco Lake, Galápagos. *Org. Geochem.* **38**, 1459-1478 (2007).

9. Zhang, Z. & Sachs, J. P. Hydrogen isotope fractionation in freshwater algae: I. Variations among lipids and species. *Org. Geochem.* **38**, 582-608 (2007).

10. Smittenberg, R. H. & Sachs, J. P. Purification of dinosterol for hydrogen isotopic analysis using high-performance liquid chromatography-mass spectrometry. *J. Chromatogr. A* **1169**, 70-76 (2007).

11. Sachse, D., Radke, J., & Gleixner, G. Hydrogen isotope ratios of recent lacustrine sedimentary *n*-alkanes record modern climate variability. *Geochim. et Cosmochim. Acta* **68**, 4877-4889 (2004).

12. Schidlowski, M., Matzigkeit, U., & Krumbein, W. E. Superheavy Organic-Carbon from Hypersaline Microbial Mats - Assimilatory Pathway and Geochemical Implications. *Naturwissenschaften* 71, 303-308 (1984).

13. Lazar, B. & Erez, J. Carbon Geochemistry of Marine-Derived Brines: I. ^{13}C depletions due to intense photosynthesis. *Geochim. Cosmochim. Acta* **56**, 335-345 (1992).

14. Trichet, J., Defarge, C., Tribble, J., Tribble, G., & Sansone, F. Christmas Island lagoonal lakes, models for the deposition of carbonate-evaporite-organic laminated sediments. *Sed. Geol.* **140**, 177-189 (2001).

15. Englebrecht, A. C. & Sachs, J. P., Determination of sediment provenance at drift sites using hydrogen isotopes and unsaturation ratios in alkenones. *Geochim. Cosmochim. Acta* **69**, 4253-4265 (2005).

16. Sessions, A. L., Burgoyne, T. W., Schimmelmann, A., & Hayes, J. M. Fractionation of hydrogen isotopes in lipid biosynthesis. *Org. Geochem.* **30**, 1193-1200 (1999).

17. Volkman, J. K. et al. Microalgal biomarkers: A review of recent research developments. *Org. Geochem.* **29**, 1163-1179 (1998).

DOI: 10.1038/NGEO554

18. Schouten, S. et al. The effect of temperature, salinity and growth rate on the stable hydrogen isotopic composition of long chain alkenones produced by *Emiliania huxleyi* and *Gephyrocapsa oceanica*. *Biogeosciences* **3**, 113-119 (2006).

19. Gat, J. R. Oxygen and hydrogen isotopes in the hydrologic cycle. *Ann. Rev. Earth Planet. Sci.* **24**, 225-262 (1996).

20. University of East Anglia. "Southern Oscillation Index Instrumental Data" (http://www.cru.uea.ac.uk/cru/data/soi.htm) (2004)

21. Hughen K.A. et al. Marine04 Marine radiocarbon age calibration, 26 - 0 ka BP. *Radiocarbon* **46,** 1059-1086 (2004).

22. Druffel, E. R. M. Bomb radiocarbon in the Pacific: Annual and seasonal timescale variations, *J. of Marine Research* **45,** 667-698 (1987).